Chapter 5: Coupling into the Base Pair Stack is Necessary for DNA-Mediated Electrochemistry

Adapted from: Gorodetsky, A. A., Green, O., Yavin, E., Barton, J. K. (2007)

Bioconjugate Chem. 18, 1434–1441.

Iodoanthraquinone was synthesized by Omar Green, and oligonucleotides containing the TEMPO label were prepared by Eylon Yavin.

ABSTRACT

The electrochemistry of DNA films modified with different redox probes linked to DNA through saturated and conjugated tethers was investigated. Experiments feature two redox probes bound to DNA on two surfaces: anthraquinone (AQ)-modified uridines incorporated into thiolated DNA on gold (Au) and 2,2,6,6-tetramethylpiperidine 1-oxyl (TEMPO)-modified uridines in pyrene-labeled DNA on highly oriented pyrolytic graphite (HOPG). The electrochemistry of these labels when incorporated into DNA has been examined in DNA films containing both well-matched and mismatched DNA. DNA-mediated electrochemistry is found to be effective for the TEMPO probe linked with an acetylene linker but not for a saturated TEMPO connected through an ethylenediamine linker. For the AQ probe, DNA-mediated electrochemistry is found with an acetylene linker to uridine but not with an alkyl chain to the 5' terminus of the oligonucleotide. Large electrochemical signals and effective discrimination of intervening base mismatches are achieved for the probes connected through the acetylene linkages, while probes connected through saturated linkages exhibit small electrochemical signals associated only with direct surface-to-probe charge transfer and poor mismatch discrimination. Thus DNA electrochemistry with these probes is dramatically influenced by the chemical nature of their linkage to DNA. These results highlight the importance of effective coupling into the π-stack for long-range DNA-mediated electrochemistry.

5.1 Introduction

Numerous studies in solution have shown that the DNA duplex can serve as an effective medium to transport charge (1–5). DNA-mediated charge transport (CT) in solution exhibits exquisite sensitivity to perturbations in the intervening base stack such as single base mismatches (6), bulges (7, 8), and protein binding (9–11). Previous work has shown that self-assembled DNA monolayers on both gold and graphite can also mediate charge transport over significant distances (12–14). In particular, electrochemistry at DNA-modified electrodes has been demonstrated in both a chip-based format for mismatch detection (15, 16, 17) and as a tool for monitoring protein/DNA interactions (18–23).

Assays based on DNA CT have frequently made use of solution-borne substrates that interact with duplex DNA at the electrode surface (12–15). To further develop electrochemical detection strategies based on DNA CT, it is necessary to explore electroactive probes that are covalently tethered to duplex DNA. Electrochemistry of DNA monolayers modified with daunomycin, ferrocene, methylene blue, and anthraquinone has shown that these redox-active reporters covalently linked to DNA can function as DNA-bound electrochemical probes (24–34). However, important questions remain regarding the nature of charge transfer to these probes, which may proceed either via the base pair stack of DNA or by direct contact of the probe with the surface.

Daunomycin has displayed particularly large electrochemical signals when used as a covalently attached probe (24–26). The size of the signals associated with this probe likely reflect its intimate intercalation within the base pair stack (35, 36), as can be seen

in crystal structures of daunomycin bound to DNA. Furthermore, breaks in the sugar phosphate backbone were shown to have no significant effect on the electrochemistry of covalently attached daunomycin (26); base mismatches, on the other hand, cause a dramatic attenuation of the signal (24). These observations are consistent with DNA CT occurring through the base pair stack rather than through the sugar-phosphate backbone.

Ferrocene/DNA conjugates have been employed in DNA electrochemistry experiments and, in particular, to examine the importance of the linkage between DNA and the redox active probe (27). Interrupting conjugation of the ferrocene label with the base pair stack results in an almost complete loss of the electrochemical signal. Furthermore, the location of the ferrocene label within a DNA monolayer was found to affect dramatically the magnitude of the electrochemical signals (29, 31). A well coupled ferrocene-uridine derivative exhibited a larger electrochemical signal at the top of the DNA monolayer than in close proximity to the surface (29). However, the opposite effect was observed for a poorly coupled ferrocene; an alkyl chain-derivatized ferrocene connected to the top of a DNA monolayer exhibited a smaller signal than the same ferrocene moiety incorporated in close proximity to the surface (31).

There remains some controversy about the effects of DNA conformation on electrochemical behavior of ferrocene, however. Recently, Anne and Demaille explored the electrochemistry of a ferrocene label attached to the 5' terminus of duplex DNA (37). These ferrocene labels were not conjugated into the base pair stack but still afforded strong electrochemical signals. Elastic bending of 5' ferrocene-labeled DNA was suggested as the cause of the electrochemical signals observed. It was concluded that bending of the DNA could account for the electrochemistry of all DNA-bound probes.

This conclusion was in direct contrast to those based upon the ferrocene data already described (29, 31). Further, these investigations did not account for the role of the linkage between DNA and ferrocene, nor the effect of sequence context on electrochemical signals.

Experiments with covalently tethered methylene blue have underscored the importance of intercalative stacking for DNA-mediated electrochemistry (28). In low salt buffers, intercalation is detected electrochemically in DNA films containing methylene blue tethered distally at the top of the film. Simply changing to a high ionic strength buffer leads to the complete loss of electrochemical signal in the DNA film; methylene blue, though still covalently attached, cannot bind by intercalation under these conditions. Thus intercalative stacking appears necessary for efficient reduction of the attached probe by DNA-mediated CT. Notably, recent studies have also demonstrated the effectiveness of methylene blue in assays based on surface-to-probe charge transfer without DNA mediation (38, 39).

In this work we focus on two established probes of DNA CT to explore in more detail how the linkage to DNA affects the efficiency of DNA-mediated electrochemistry. We have utilized two different redox active markers that can be covalently attached to DNA. Anthraquinone (AQ) has been extensively studied in electrochemical assays based on DNA-mediated CT. For example, AQ has been applied to the electrochemical monitoring of primer extension reactions at Au surfaces (29). Additionally, AQ-modified uridines have been used for detection of single nucleotide polymorphisms (32, 33) and of duplex-to-triplex conversions at DNA-modified Au surfaces (34). Recent studies in our group have also examined uridine modified with 2,2,6,6-tetramethyl-3,4-

dehydro-piperidine-N-oxyl (3,4-dehydro-TEMPO) as a probe of DNA CT from a redox-active protein to DNA (40). Notably, the acetylene linkage connecting the probe to the uridine was shown to be crucial for determining its effectiveness as an electron trap for DNA CT using electron paramagnetic resonance (EPR) spectroscopy.

Here we present the electrochemistry of DNA duplexes featuring AQ-modified uridines on Au and TEMPO-modified uridines on highly oriented pyrolytic graphite (HOPG). The observations reported for the AQ and TEMPO probes make them particularly well suited for establishing a correlation between the linkage connecting the probe to the DNA and the effectiveness of the probe in assays based on DNA-mediated electrochemistry. On DNA-modified HOPG, we examine the difference between a modified 3,4-dehydro-TEMPO moiety connected to the base pair stack via an acetylene linker and a saturated TEMPO connected via an ethylenediamine linker. On DNA-modified Au, we examine the difference between an AQ moiety connected to the base pair stack via an acetylene linker and an AQ linked via an alkyl chain to the 5' terminus of the DNA. Electrochemistry with these probes is dramatically influenced by the chemical nature of their linkage to DNA.

5.2 Experimental Section

5.2.1 Materials

All phosphoramidites and reagents for DNA synthesis were purchased from Glen Research with the exception of the 5-ethynyluracil phosphoramidite, which was purchased from Berry and Associates. All organic reagents (acetonitrile,

dichloromethane, N,N-dimethylformamide, pyridine, tetrahydrofuran, triethylamine, and 40% aqueous methylamine solution) were purchased from Aldrich in the highest available purity and used as received. All buffers were freshly prepared and filtered using a 0.45 μm filter prior to use. Tetrakis(triphenylphosphine)Pd(0) was purchased from Strem Chemicals. Technical grade 2-aminoanthraquinone was obtained from Aldrich, and anthraquinone-2-carbonyl chloride was purchased from TCI America. The synthesis of 2-iodoanthraquinone has been previously described (41). TEMPO was purchased from Aldrich. The preparation of 4-diamoethylene-2,2,6,6-tetramethyl-3,4-dehydropiperidine-N-oxyl (ethylenediamine TEMPO) (42) and 4-ethynyl-2,2,6,6-tetramethyl-3,4-dehydropiperidine-N-oxyl (acetylene-3,4-dehydro-TEMPO) (40, 43) followed established literature procedures.

5.2.2 Oligonucleotide Synthesis

Oligonucleotides were prepared using standard phosphoramidite chemistry on an ABI 392 DNA Synthesizer. DNA was purified by HPLC on a reverse phase C18 column with acetonitrile and ammonium acetate as the eluents. Unless otherwise noted, all oligonucleotides were cleaved from the resin with concentrated ammonium hydroxide (NH_4OH) prior to purification. The desired products were characterized by UV-visible spectroscopy and MALDI-TOF mass spectrometry.

5.2.3 Synthesis of Pyrene-Modified Oligonucleotides

DNA was modified with pyrene at the 5' terminus by following a previously reported procedure (13). In brief, oligonucleotides were prepared by solid-phase synthesis with an unprotected hydroxyl group at the 5' terminus. The 5'-OH was treated with a 120 mg/mL solution of carbonyldiimidazole in dioxane for 2 hours followed by

an 80 mg/mL solution of 1,6-diaminohexane for 30 min. Subsequently, the free amine was treated with 1-pyrenebutyric acid, N-hydroxysuccinimide ester, resulting in the desired pyrene moiety linked to the 5' terminus. The oligonucleotides were deprotected with concentrated NH_4OH at 60 ºC for 6 hours.

5.2.4 Synthesis of Thiol-Modified Oligonucleotides

The synthesis of DNA featuring a thiol at the 5' terminus followed previously established procedures (44). In brief, oligonucleotides were prepared by solid-phase synthesis with the commercially available C6 S-S linker phosphoramidite incorporated at the 5' terminus. The oligonucleotides were deprotected in NH_4OH at 60 °C for 12 h. Dithiothreitol (100 mM) was subsequently added to reduce the disulfide, leaving a free thiol at the 5' terminus.

5.2.5 Synthesis of TEMPO-Modified Oligonucleotides

The synthesis of acetylene 3,4-dehydro-TEMPO-modified DNA has been previously described (40). The 5' DMT-protected 5-iodouridine was Pd coupled to the acetylene-modified 3,4-dehydro-TEMPO in THF. The 3'-OH of the product of this reaction was subsequently converted to its phosphoramidite form. The phosphoramidite was dissolved in acetonitrile and used immediately for DNA synthesis.

The synthesis of the ethylenediamine TEMPO-modified DNA was carried out according to a protocol adapted from the literature (42). DNA featuring a 5-bromouridine at the position targeted for modification was synthesized on a solid support. A ~ 0.5 M aqueous solution of the ethylenediamine TEMPO was added to the 5-bromouridine-modified DNA on solid support with the resulting slurry incubated at 60 ºC overnight. This incubation resulted in the ethylenediamine TEMPO replacing the

bromine, and in cleaving the DNA from the bead and deprotecting the bases. Prior to HPLC purification, the aqueous phase was washed with dichloromethane to remove excess ethylenediamine TEMPO.

5.2.6 Synthesis of Anthraquinone-Modified Oligonucleotides

The modification of DNA with anthraquinone was carried out as shown in Scheme 5.1. 2-Iodoanthraquinone was synthesized according to literature precedent (41). DNA containing a 5-ethynyluracil at the position targeted for modification was synthesized on a solid support. The beads were placed in an oven-dried flask which had been charged with 2.5 mL of DMF/Et_3N (3.5:1.5). 2-Iodoanthraquinone (60 mmol) and CuI (60 mmol) were added to the flask, and the solution was flushed with argon. $Pd(PPh_3)_4$ (30 mmol) was then added to the flask, and the solution was again flushed with argon. The mixture was allowed to stir at ambient temperature for 3 hours under argon. Subsequently, the beads were washed with a 5% (w/v) EDTA solution, DMF, CH_3CN, and CH_2Cl_2 in succession to remove excess reagents. The DNA was cleaved from the resin and deprotected at 60 ºC for 20 minutes with a 1:1 mixture of 40% aqueous methylamine and a saturated ammonium hydroxide solution. m/z calculated 5417, found 5416. λ_{max} nm (M^{-1} cm^{-1}) 260 (ε 158 400), 320 (ε 58 000), 394 (ε 43 800).

Attachment of AQ at the 5' terminus of DNA was carried out using procedures modified from the literature and Glen Research protocols (44-47). DNA with a six-methyl carbon chain terminated with a monomethoxytrityl (MMT)-protected amine was incorporated at the 5' terminus on the solid support. The MMT-protecting group was removed from the 5' amine with 3% trichloroacetic acid in CH_2Cl_2. A 0.5 M solution of

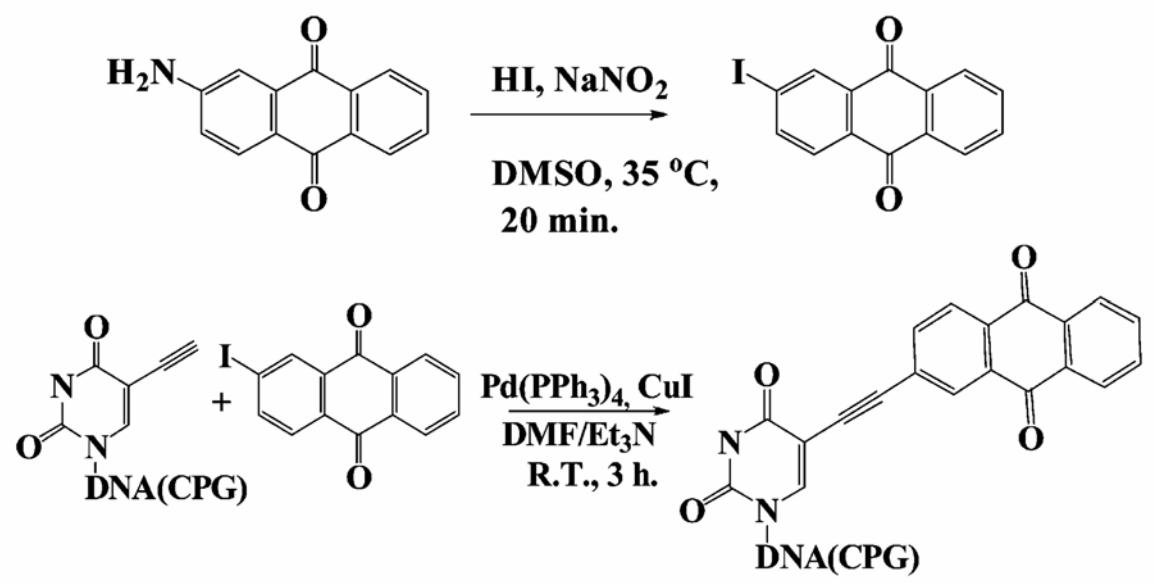

Scheme 5.1: Conditions for synthesis of 2-Iodoanthraquinone and its coupling to ethynyluracil-modified DNA. The synthesis of 2-iodoanthraquinone was performed according to literature procedure (41). The coupling of the 2-iodoanthraquinone to the ethynyluracil-modified DNA was performed while the DNA was still attached to controlled pore glass (CPG) solid support.

anthraquinone-2-carbonyl chloride in CH_2Cl_2/Et_3N (10:1) was added to the amine-modified DNA on solid support. The resulting slurry was incubated overnight. The beads were subsequently washed with copious amounts of CH_2Cl_2 to remove excess reagents. The DNA was cleaved from the resin at 60 ºC for 20 minutes with a 1:1 mixture of 40% aqueous methylamine and a saturated ammonium hydroxide solution. *m*/*z* calculated 5615, found 5614.

5.2.7 Formation of DNA Monolayers

DNA films were formed on SPI-1 grade HOPG electrodes (SPI, Inc.) with a surface area of 0.08 cm^2, or on commercially available Au electrodes (BAS, Inc.) with a surface area of 0.02 cm^2, as previously described (12, 13). Duplex DNA (in 5 mM sodium phosphate, 50 mM NaCl, pH 7.1) was formed by combining equimolar amounts of the pyrene or thiol-modified strand with TEMPO or AQ-labeled complements, respectively. Duplex DNA (25-50 μM) was deposited onto HOPG or Au over a period of 24-48 hours. Mg^{2+} was included to minimize electrostatic repulsion between the duplexes and ensure well-packed monolayers on both HOPG and Au (12, 13). Longer incubation times (48 hours) and lower incubation temperatures (4 ºC) generally improved film formation. Electrodes being compared were prepared under equivalent conditions. Also, electrodes were brought to ambient temperature prior to electrochemical analysis.

5.2.8 Electrochemical Measurements

Electrochemical data were collected using a CH Instruments 760B potentiostat. Electrochemical experiments were performed at ambient temperature in 5 mM sodium phosphate, 50 mM NaCl, pH 7.1, under anaerobic conditions. All measurements

reported for working electrodes were taken versus a platinum (Pt) auxiliary. Either a saturated calomel electrode or a silver/silver chloride electrode (Ag/AgCl) was used as the reference electrode. Square wave voltammetry was performed at 15 Hz, and cyclic voltammetry was performed at 50 mV/s.

5.2.9 Surface Characterization

All atomic force microscopy (AFM) measurements were performed using an MFP-3D atomic force microscope from Asylum Research, Inc. (Santa Barbara, CA). The HOPG block was mounted in a custom designed glass chamber before being modified with DNA as described. AFM measurements were performed in buffer containing 5 mM sodium phosphate, 50 mM NaCl, pH 7.1, either in contact (constant force) or tapping mode. Commercially available silicon tips were utilized for all experiments.

5.3 Results

5.3.1 Electrochemical Probes and DNA Sequences

The electrochemical probes and sequences examined are illustrated in Figure 5.1. Two redox active probes were tested, AQ and TEMPO-based moieties, and the probes were each linked to the base pair stack in two ways. The AQ was attached to a modified uridine via an acetylene linker and to the 5' phosphate terminus via a six-carbon alkane linker. The synthesis of the acetylene-linked AQ moiety involved coupling of 2-iodoanthraquinone to ethylnyl-modified DNA (Scheme 5.1). Although DNA has previously been modified via Sonogashira conditions (48, 49), these syntheses involved

halogenated bases incorporated into DNA coupled to ethynyl-containing molecules. 3,4-Dehydro-TEMPO was attached to a modified uridine by an acetylene linker, and TEMPO was connected via an ethylenediamine linker. The acetylene linkage and the 3,4-dehydro-TEMPO probe were designed to allow for efficient coupling of the probe into the base pair stack, whereas the alkane linkage was intended to insulate the probe electronically from the base pair stack. TEMPO experiments were performed with a 15-mer sequence modified with a pyrene on the complementary strand. The 15-mer sequence selected to compare the acetylene and saturated TEMPO probes is that utilized extensively by our laboratory (12, 15) and others (27) in characterizing different redox probes for DNA-mediated redox chemistry. Many experiments have been used to demonstrate, however, for a variety of probes that DNA-mediated electrochemistry is independent of DNA sequence and length (< 30 bp) (12, 13, 15, 18, 24–26). It should be noted that electrochemistry experiments were also carried out on the 10-mer TEMPO probes that had been utilized in solution experiments with similar results (data not shown) (40). Anthraquinone experiments are described using a 17-mer oligonucleotide sequence containing a 5'-thiolate on the strand complementary to that modified with AQ. Several different AQ-modified DNA sequences 14–17 base pairs in length were prepared with comparable results obtained. Since neither of these redox probes intercalate directly into the DNA base stack, they depend upon their links to the stacked uridine within the helix for π-coupling. Hence parallel experiments with these assemblies should give insight into the effect of DNA-probe linkages on DNA-mediated electrochemistry.

Two different surfaces, Au and graphite, are utilized for these electrochemical experiments. Studies involving AQ-modified DNA were performed on standard Au

electrodes since the aromatic AQ moiety may directly adsorb to the graphite surface, impeding proper formation of DNA monolayers. Experiments utilizing TEMPO-modified DNA take advantage of the extended potential range afforded by HOPG. Since thiols are known to undergo oxidation at the large positive biases necessary for oxidation of TEMPO, HOPG is more suitable for exploring the electrochemistry of this marker.

Electrochemical measurements were used to assess the CT yields from the surface to the redox active probe. The efficiency of DNA CT was determined by direct comparison of peak currents and integrated charge obtained using square wave and cyclic voltammetry. Peak potentials were obtained using SWV and are reported versus NHE.

5.3.2 Electrochemistry of the Acetylene-Linked Probes

Large electrochemical signals are observed for probes linked to the DNA via an acetylene unit. Figure 5.2 shows the SWV of the acetylene-linked AQ and TEMPO moieties. A reversible electrochemical signal is found at -301 (±7) mV versus NHE for AQ-modified DNA on Au, and the signal is stable for a minimum of two hundred scans under anaerobic conditions. The magnitudes and potentials of the AQ signals are similar to those previously reported (29-34). As expected for a surface-bound species, a plot of peak current as a function of scan rate is linear for the DNA-bound AQ as shown in Figure 5.3 (50), and the electron-transfer rate was estimated to be approximately 30 s^{-1}. This electron-transfer rate is consistent with previous electrochemical studies of DNA-modified surfaces using similar alkylthiol linkages to bind the DNA to the Au surface (24, 26). A reversible electrochemical signal is also observed at 810 (±20) mV versus

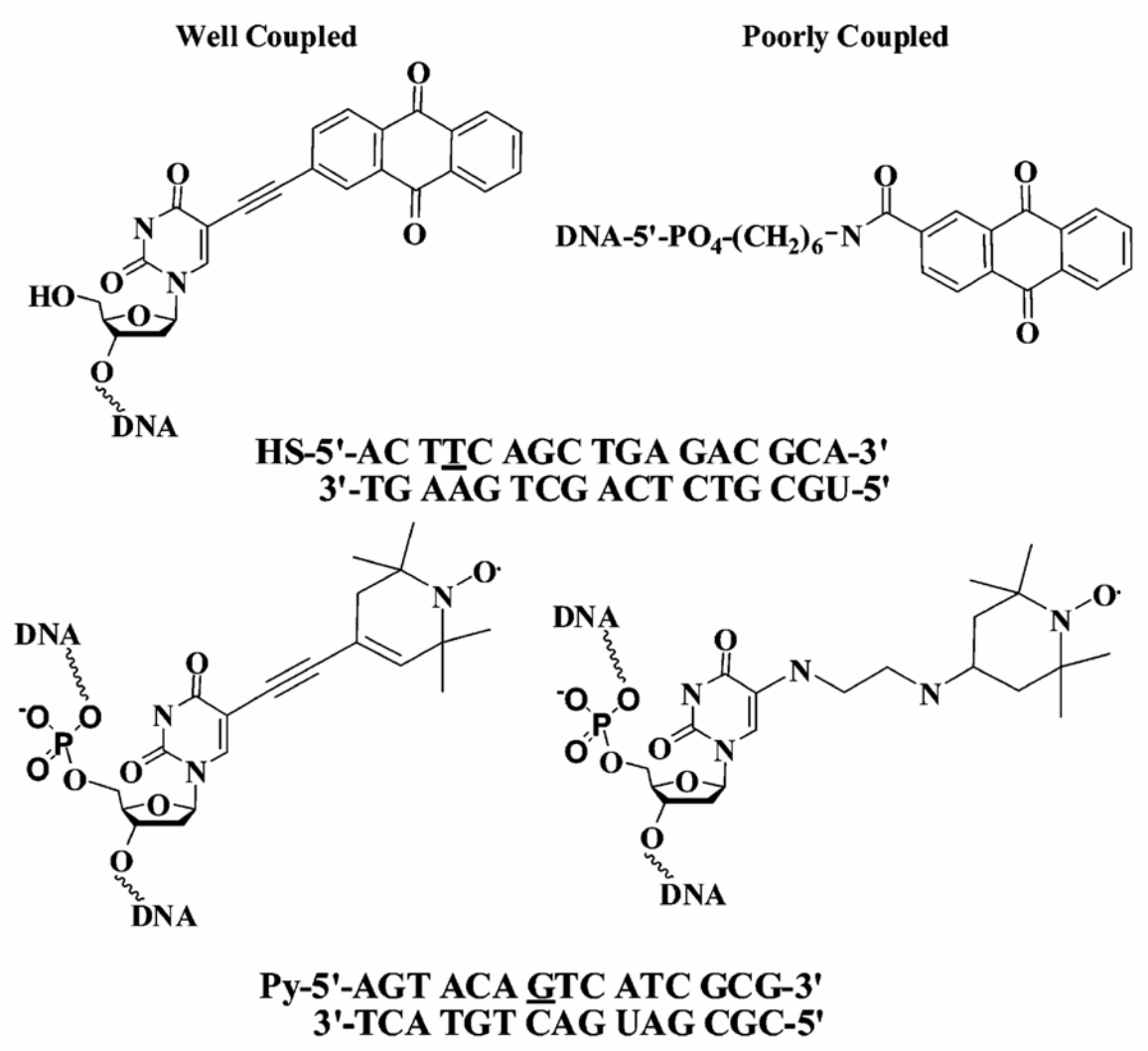

Figure 5.1: Sequences and probes used during the course of these studies. The DNA sequence used for each electrochemical marker is shown below the structures of the markers. Top: structures of well- and poorly coupled AQ; -SH indicates the position of thiol modification on DNA. Bottom: structures of well- and poorly coupled TEMPO and its derivative; Py- indicates the position of pyrene modification on DNA. The location of the mismatch is underlined, and the location of the electrochemical probe is indicated by uracil (U).

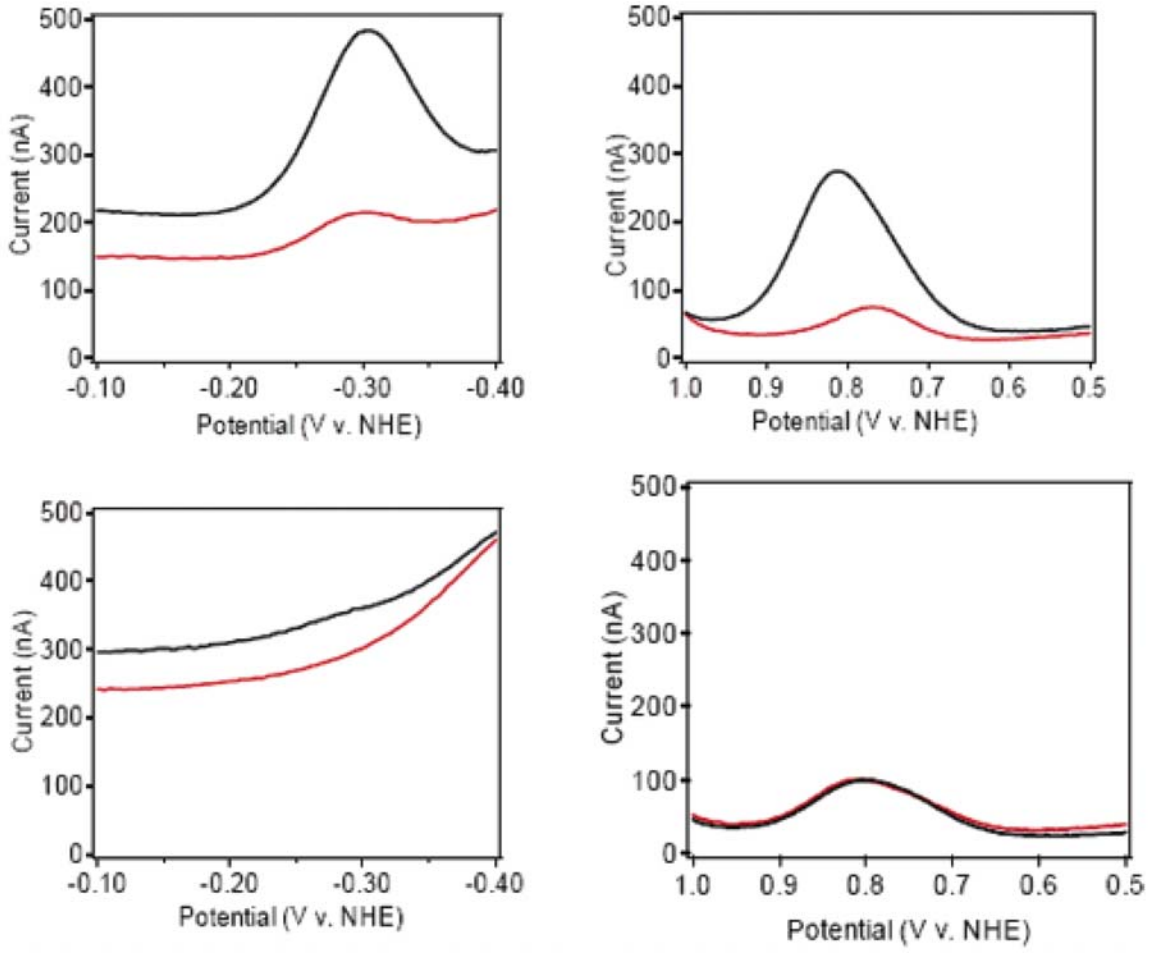

Figure 5.2: Square wave voltammetry of AQ and TEMPO-modified DNA. Voltammograms for DNA modified with the acetylene-linked AQ (top left), the acetylene-linked 3,4-dehydro-TEMPO (top right), the alkane-linked AQ (bottom left), and the alkane-linked TEMPO (bottom right) are shown. Voltammograms of well-matched DNA are shown in black, and voltammograms of DNA featuring a CA mismatch are shown in red. All experiments were performed in 5 mM sodium phosphate, 50 mM NaCl, pH 7.1 buffer.

A.

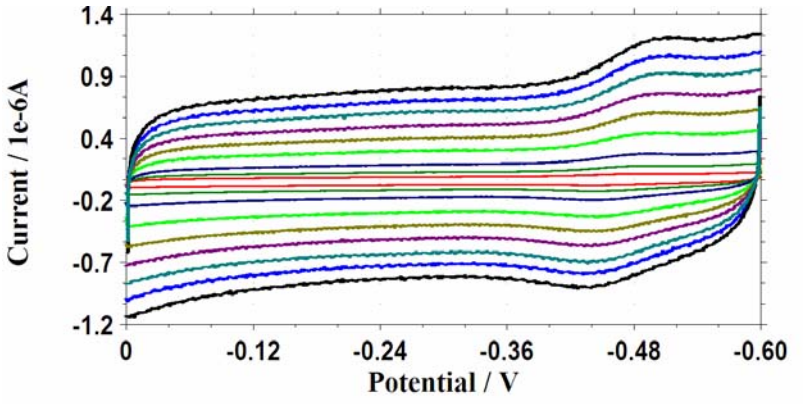

B.

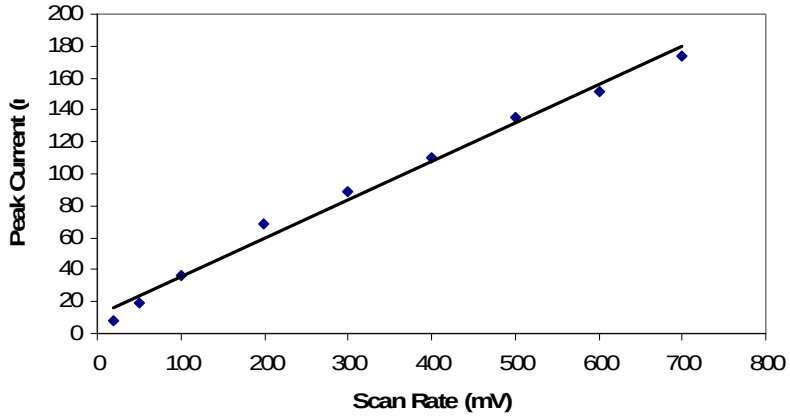

Figure 5.3: Cyclic voltammetry of AQ-modified DNA at various scan rates (A) and the corresponding plot of peak current as a function of scan rate (B). The experiment was performed in 5 mM sodium phosphate, 50 mM NaCl, pH 7.1 buffer.

NHE for the 3,4-dehydro-TEMPO-modified DNA on graphite. The potential of the signal observed for the 3,4-dehydro-TEMPO-modified DNA is similar to that previously reported for the free label in solution (40). It is important to note that the TEMPO signal is electrochemically unstable and rapidly decays upon repeated scanning when attached to an electrode or to graphite felt (51, 52). Therefore, a plot of peak current as a function of scan rate could not be easily obtained for this marker. As expected, controls run with well-matched, unmodified DNA reveal no electrochemical signals at the potentials reported for the 3,4-dehydro-TEMPO and AQ-modified DNA.

The introduction of a mismatch below the two labels causes a significant attenuation of the electrochemical signal (Figure 5.2 and Table 5.1). For AQ-modified DNA, the peak current is reduced from 160 (±50) nA for well-matched DNA to 40 (±20) nA for DNA featuring a CA mismatch. For the 3,4-dehydro-TEMPO-modified DNA, the peak current is reduced from 250 (±100) nA for well-matched DNA to 30 (±15) nA for DNA featuring a CA mismatch below the probe. It is noteworthy that the introduction of a CA mismatch above the 3,4-dehydro-TEMPO probe has little effect on the magnitude of the peak current (Figure 5.4).

5.3.3 Electrochemistry of the Poorly Coupled Probes

Small electrochemical signals are observed for probes connected to the DNA via an alkane linkage. Figure 5.2 also shows SWVs for the alkane-linked AQ and TEMPO moieties. A small signal centered at -330 (±60) mV versus NHE, whose reversibility cannot be judged, is observed for the AQ-modified DNA on Au. The size of this signal makes it difficult to obtain a plot of peak current as a function of scan rate. The signal is reduced by almost 2 orders of magnitude in comparison to the acetylene-linked AQ

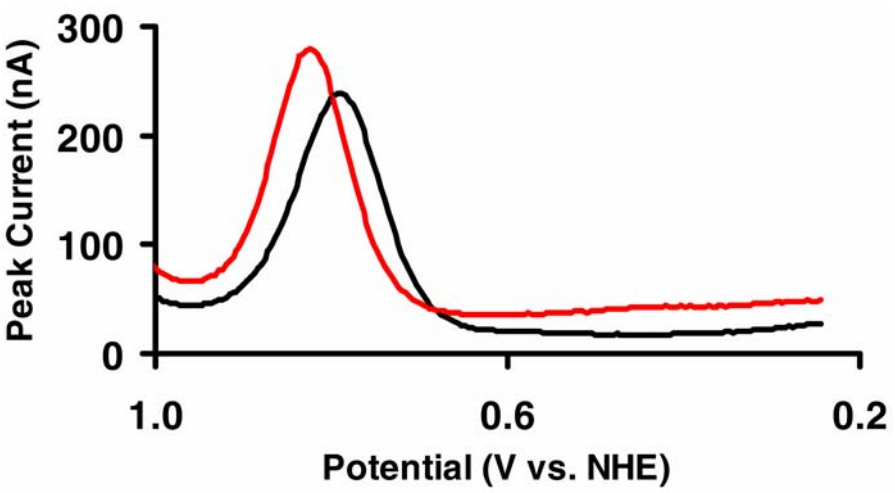

Figure 5.4: Square wave voltammetry of a surface featuring well-matched DNA modified with an acetylene-TEMPO label (black) and DNA with a CA mismatch above the acetylene-TEMPO label (red). The sequence was pyrene-$(CH_2)_3CONH(CH_2)_6NHCO$-5'-CTA C*A*G **T**CG T-3' where the italicized base indicates the location of the TEMPO and the bold base indicates the location of the mismatch. The experiments were performed in 5 mM sodium phosphate, 50 mM NaCl, pH 7.1 buffer.

DNA sequence[a]	AQ[a] peak current[b] (nA)	AQ[a] potential[c] (mV)	TEMPO[a] peak current[b] (nA)	TEMPO[a] potential[c] (mV)
well coupled	160 (±50)	−301 (±7)	250 (±100)[d]	810 (±20)[d]
CA mismatch	40 (±20)	−302 (±8)	34 (±15)[d]	800 (±50)[d]
poorly coupled	9 (±4)	−330 (±60)	64 (±17)	800 (±11)

[a] See Figure 1 for structures and sequences. Well coupled and CA mismatch DNA sequences contain sequences with marker moieties attached to the DNA through an ethynyl linkage. Well coupled DNA strands are fully complementary, and CA mismatch strands contain a CA mismatch at the position indicated in Figure 1. Poorly coupled DNA sequences have the electroactive molecule coupled through a saturated linkage, as shown in Figure 1. [b] Peak currents are reported from square wave voltammetry (SWV). SWV was performed at 15 Hz in 5 mM sodium phosphate, 50 mM NaCl, pH 7.1, under anaerobic conditions. Electrochemical data were compiled over a minimum of five trials. Experiments were performed with a SCE reference electrode and a Pt wire auxiliary electrode. [c] All electrochemical potentials are reported vs NHE. [d] DNA modified with 3,4-dehydro-TEMPO.

Table 5.1: Electrochemical characteristics of DNA monolayers modified with electroactive moieties

probe (Table 5.1) with a drop in peak current from 160 (±50) nA to 9 (±4) nA. For the ethylenediamine-linked TEMPO label, a reversible signal is found at 800 (±10) mV versus NHE. Unlike the AQ, the magnitude of the TEMPO signal is reduced by only 4-fold upon altering the linkage from an acetylene to an alkane; the peak current drops from 250 (±100) nA for the acetylene-linked 3,4-dehydro-TEMPO to 60 (±20) nA for the ethylenediamine-linked TEMPO. As with the AQ case, the smaller size and instability of the TEMPO signal make it difficult to plot peak current as a function of scan rate.

In contrast to that seen for the acetylene-linked probes, the introduction of a mismatch below the alkane-linked AQ and TEMPO labels does not lead to substantial reductions in the electrochemical signals (Figure 5.2). Incorporation of a CA mismatch below the alkane AQ has virtually no effect on the electrochemical signal. The electrochemical signals are small for both well-matched and mismatched DNA making quantitative evaluation difficult. Similarly, incorporation of a CA mismatch below the ethylenediamine-linked TEMPO does not lead to a diminution in the electrochemical signal. Well-defined electrochemical signals are observed with and without the mismatches for these ethylenediamine-linked, TEMPO-modified DNAs. Peak currents of 60 (±20) nA are found for well-matched TEMPO-modified DNA, and peak currents of 70 (±10) nA are found for DNA featuring a CA mismatch below the TEMPO.

5.3.4 Surface Characterization

To aid in the proper interpretation of electrochemical data, surface characterization is necessary. DNA monolayers on both HOPG and Au have previously been examined using scanning probe microscopy, radioactive labeling, and

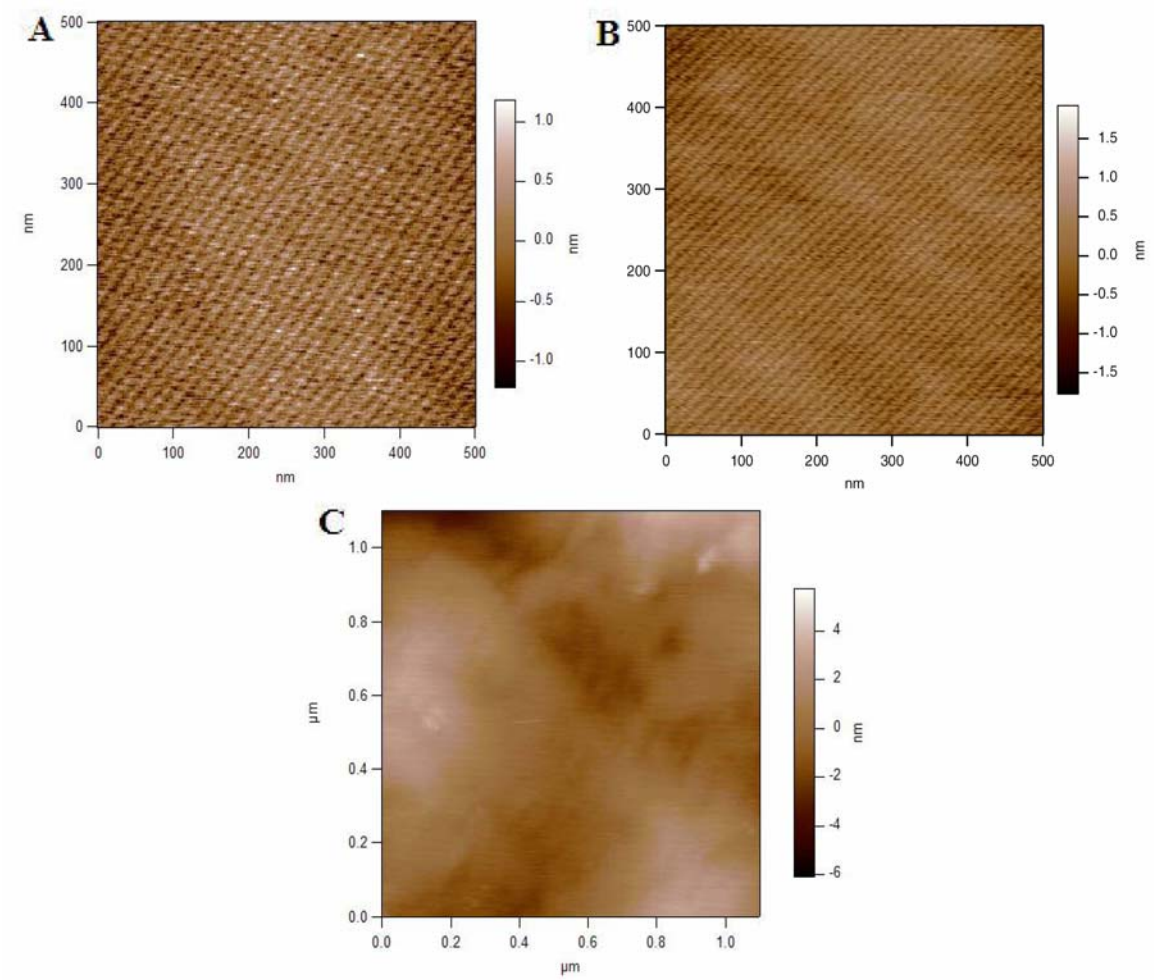

Figure 5.5: Tapping mode AFM characterization of DNA-modified and bare HOPG in 5 mM sodium phosphate, 50 mM NaCl, pH 7.1 buffer. (A) Well-matched and unmodified DNA on HOPG. (B) Well-matched DNA featuring an acetylene-TEMPO uridine. (C) Unmodified HOPG. The sequences were pyrene-$(CH_2)_3CONH(CH_2)_6NHCO$-5'-CTA C*A*G TCG T-3' plus unmodified complement (A) or plus TEMPO modified complement (B).

electrochemical techniques (13, 53, 54, 55). Previous AFM measurements found smooth films with depths corresponding to duplexes oriented at a ~45° angle with respect to the surface. As a complement to our electrochemical studies, we also examined DNA monolayers with or without appended electrochemical markers on HOPG (Figure 5.5). These monolayers were found to be indistinguishable from those previously examined.

5.4 Discussion

5.4.1 Electrochemical Reduction of the Acetylene-Linked Probes Is Mediated by the DNA Duplex

For efficient DNA-mediated CT, it is necessary for the electrochemical probe to be directly coupled into the base pair stack. Our data provide strong evidence that the acetylene-linked probes are reduced in a DNA-mediated fashion. The largest signals are found for 3,4-dehydro-TEMPO and AQ moieties connected to the DNA by an acetylene linker. The inclusion of a CA mismatch below either of these probes significantly attenuates the electrochemical signal, a hallmark of DNA-mediated CT.

Interestingly, previous reports of DNA modified with AQ-labeled uridines allow for a strong correlation to be drawn between the nature of the DNA-probe linkage and the size of the electrochemical signal. The signals obtained here for an unsaturated tether integrate to current densities of 7900 nA/cm^2. Gooding and co-workers have previously reported the electrochemistry of a partially saturated tether whose current densities integrate to a value of ~ 1500 nA/cm^2 (29, 30). Further, Okamoto and co-workers have found current densities on the order of ~ 300 nA/cm^2 for a fully saturated linkage (32,

33). A clear trend emerges from these values: a linkage which allows for conjugation of the probe into the π-stack leads to larger redox signals and more effective electrochemistry.

DNA-mediated electrochemistry is observed for the acetylene-linked probes at both positive and negative potentials. DNA is expected to be repelled from the surface at negative potentials and attracted to the surface at positive potentials (53, 56). Assays based on DNA-mediated electrochemistry rely on DNA maintaining an upright orientation; CT can then take place through the base pair stack. However, at positive potentials direct contact of the probe with the surface is possible if sufficient space surrounding each duplex is available. It has been shown that in a close-packed monolayer, the DNA is not able to make direct contact with the surface (56). Therefore, assays based on DNA CT may be possible even for probes which are reduced at positive potentials.

5.4.2 Electrochemical Reduction of Alkane-Linked Probes Do Not Depend on DNA Mediated Electrochemistry

Electrochemical experiments with alkane-tethered TEMPO and AQ labels support the notion of direct surface-to-probe charge transfer for these assemblies. Changing from an acetylene linkage to an alkane linkage minimizes electronic coupling, and the signals observed for such linkages are associated with pathways of charge-transfer that are not DNA-mediated. The lack of mismatch discrimination observed for either of these probes strongly supports the notion of direct surface-to-probe CT for these cases. Since there is no effect upon inclusion of a mismatch in the DNA sequence, this electrochemistry cannot be mediated by the base pair stack.

The current densities obtained for the alkane-linked TEMPO and AQ labels are much smaller than those of the acetylene-linked probes. The peak current densities obtained from SWV are 400 nA/cm^2 and 200 nA/cm^2 for the TEMPO and AQ, respectively. Anthraquinone is a poor intercalator which should not interact strongly with the base pair stack, and TEMPO does not intercalate. Therefore the smaller signals for these probes are reasonable since the CT pathway to each of these probes involves poor electronic coupling. Furthermore, it is not unexpected that the TEMPO label exhibits larger current densities compared to the AQ label. The AQ is reduced at negative potentials, where DNA is repelled from the surface, making reduction of the probe by direct CT from the surface less likely (53, 56). On the other hand, the TEMPO is oxidized at positive potentials where the DNA can electrostatically contact the surface, making direct surface-to-probe charge-transfer more likely (53, 56).

5.4.3 Electronic Coupling into the Base Pair Stack Governs the Size of the Electrochemical Signal

Electrochemical signals that are far smaller than expected based on surface coverage are observed for the acetylene-linked probes versus that expected when compared to the electrochemical signal of intercalated daunomycin (24). Previous reports for daunomycin have revealed surface coverages of 35–45 pmol/cm^2 based upon charge integration (24, 25). These values are similar to the theoretical maximum coverage of the surface by a DNA monolayer. However, far lower apparent surface coverages are obtained for the two acetylene-linked probes presented here; cathodic waves give peak currents (Table 5.1) which roughly translate to surface coverages of 6 and 8 pmol/cm^2 for the AQ- and TEMPO-modified DNA, respectively.

How can the dramatic difference in signal intensities be reconciled? Covalently attached daunomycin has a particularly intimate association with the base pair stack and raises the melting temperature of the duplex by 20 ºC upon crosslinking (35, 36). On the other hand, the bulky AQ moiety only raises the melting temperature of the DNA duplex by 4 ºC compared to unmodified DNA. Therefore, it is reasonable to assume that the AQ is not as well coupled into the DNA base stack. This lack of electronic coupling would account for the smaller electrochemical signals observed relative to DM.

In order to investigate if the apparent discrepancy in surface coverage is due to the AQ and TEMPO moieties interfering with surface formation, the monolayers were examined by scanning probe microscopy. Previous work has shown that even subtle structural variations in the DNA monolayer can be easily detected with a high-resolution AFM tip (54). However, we observed no obvious differences between the morphology of monolayers formed with acetylene-TEMPO-modified DNA and unmodified, well matched DNA (Figure 5.5).

5.4.4 DNA Charge Transfer with Acetylene and Alkane-Linked Probes

The two linkages may provide different electron-transfer pathways from the electrode to the marker, as illustrated schematically in Figure 5.6. When the probes are effectively coupled into the base pair stack through an acetylene linkage, the yield of DNA-mediated electrochemistry is high and charge transfer through the DNA base pair stack takes place. Large electrochemical signals result, and perturbations within the base pair stack can be easily detected. When the probes are insulated from the base pair stack through a σ-bonded alkane linkage, the yield of DNA-mediated electrochemistry is low

A.

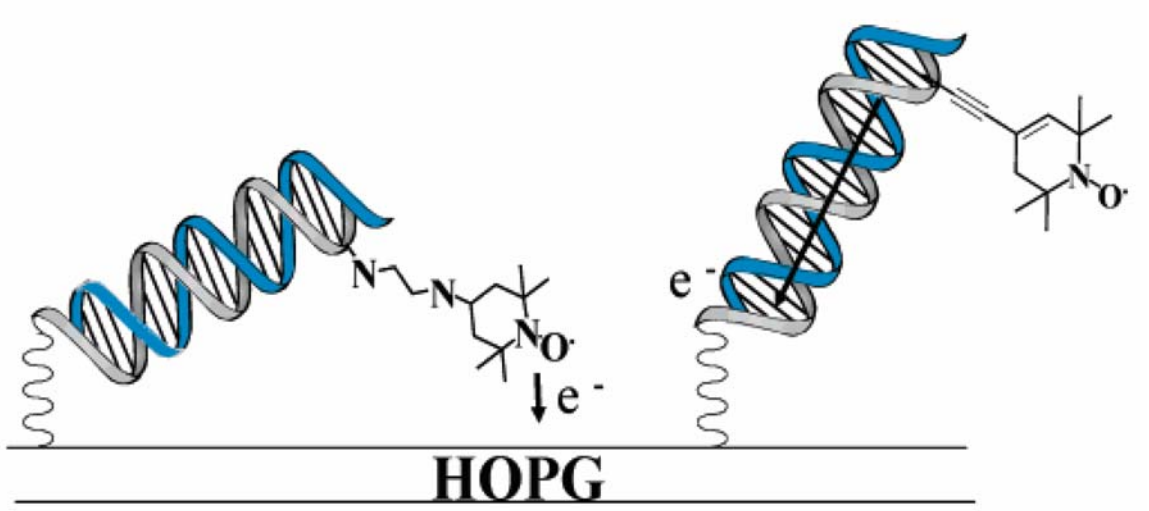

Figure 5.6: Schematic representation of two possible modes of charge transfer from an electroactive label incorporated into DNA. Direct interaction of the diaminoethane-linked TEMPO probe with the surface is shown on the left, and DNA-mediated electrochemistry to the well-coupled probe is shown on the right.

and alternative charge-transfer pathways are dominant. Small electrochemical signals are observed and perturbations within the base pair stack are not easily detected.

These results can now be used to reexamine some of the data obtained from experiments involving long-range oxidative damage to DNA. Adequate sensitivity to mismatches or lesions can only be achieved with probes that are well coupled into the DNA base pair stack. Consequently, solution studies with covalently attached anthraquinone provide a particularly interesting example of the necessity of coupling into the DNA base pair stack. For example, in direct agreement with the electrochemical data presented here, anthraquinone linked to the 5' terminus of DNA by an alkane chain has exhibited poor mismatch sensitivity in some contexts (46). Additionally, a direct comparison of the ability of various photo-oxidants to promote DNA-mediated CT showed that even changing the length of the linker connecting the anthraquinone had a significant effect on the yields of oxidative damage. In the same study, significant differences were found between poorly coupled probes that bind by an end-capping mode and well-coupled probes that bind by an intercalative mode. Therefore, it is important to note that DNA CT reveals the characteristics not only of the DNA sequence employed but also of the redox probe.

Consideration of the inherent sensitivity of DNA CT to the linkage of the redox probe to the DNA base pair stack can also be extended to solution studies of protein/DNA interactions. A uridine modified with the TEMPO moiety was utilized as an electron trap for DNA-bound repair enzymes (40). Notably, the linkage connecting the TEMPO to the uridine was shown to be crucial for determining its effectiveness as an electron trap in EPR experiments. When the TEMPO moiety is connected to a uridine

by an unsaturated acetylene linkage, large EPR signals result, consistent with the larger electrochemical signals observed for this probe. On the other hand, when the TEMPO probe is connected by a saturated linkage, smaller EPR and electrochemical signals result.

5.5 Implications

Subtle structural changes can have a significant effect on the sensitivity of redox active reporters in DNA-mediated electrochemistry. Clearly, the utility of labels that are covalently attached to DNA depends upon their interaction with the base pair stack of DNA. Assays based on DNA-mediated CT necessitate well-coupled probes that are highly sensitive to even subtle perturbations in the base pair stack.

This need is clearly illustrated by the electrochemical characteristics of AQ and TEMPO when coupled to DNA via a saturated linker versus being conjugated into the base stack. The electrochemistry of the acetylene-linked 3,4-dehydro-TEMPO and AQ is shown to be DNA-mediated. In contrast, charge transfer to the alkane TEMPO on HOPG and the alkane AQ on Au must proceed through an alternate direct surface-to-marker pathway. The data presented makes it clear that linkers conjugated into the base pair stack afford larger electrochemical signals, revealing a direct connection between the electronic structures of DNA-bound probes and their electrochemical properties.

DNA-modified electrodes are a powerful tool for directly comparing the electrochemistry of various redox active probes that are bound to DNA. DNA-mediated electrochemistry clearly allows the base pair stack to be probed directly. However,

surface-to-probe charge transfer, while useful in other contexts, does not allow for the DNA base pair stack to be interrogated. In fact, the impressive sensitivity of DNA CT chemistry allows for the transduction of small structural changes into large electrochemical differences. As observed in the current study, the linkage directly governs the electrochemical characteristics of the probe. For electrochemical assays to be successful, it is crucial to tailor the probe to the desired application.

REFERENCES

(1) Boon, E. M., Barton, J. K. (2002) *Curr. Opin. Struct. Biol. 12*, 320–329.

(2) Delaney, S., Barton, J. K. (2003) *J. Org. Chem. 68*, 6475–6483.

(3) O'Neill, M. A., Barton, J. K. (2005) *Charge Transfer in DNA: From Mechanism to Application* (H.-A. Wagenknecht), pp. 27–75, Wiley-VCH, Hoboken.

(4) Giese, B. (2000) *Acc. Chem. Res. 33*, 631–636.

(5) Schuster, G. B. (2000) *Acc. Chem. Res. 33*, 253–260.

(6) Bhattacharya, P. K., Barton, J. K. (2001) *J. Am. Chem. Soc. 123*, 8649–8656.

(7) Hall, D. B., Barton, J. K. (1997) *J. Am. Chem. Soc. 119*, 5045–5046.

(8) Dandliker, P. J., Holmlin, R. E., Barton, J. K. (1997) *Science 275*, 1465–1468.

(9) Rajski, S. R., Kumar, S., Roberts, R. J., Barton, J. K. (1999) *J. Am. Chem. Soc. 121*, 5615–5616.

(10) Rajski, S. R., Barton, J. K. (2001) *Biochemistry 40*, 5556–5564.

(11) Boon, E. M., Pope, M. A., Williams, S. D., David, S. S., Barton, J. K. (2002) *Biochemistry 41*, 8464–8470.

(12) Kelley, S. O., Boon, E. M., Barton, J. K., Jackson, N. M., Hill, M. G. (1999) *Nucl. Acids Res. 27*, 4830–4837.

(13) Gorodetsky, A. A., Barton, J. K. (2006) *Langmuir 22*, 7917–7922.

(14) Li, X., Song, H., Nakatani, K., Kraatz, H.-B. (2007) *Anal. Chem. 79*, 2552–2555.

(15) Boon, E. M., Ceres, D. M., Drummond, T. G., Hill, M. G., Barton, J. K. (2000) *Nature Biotechnol. 18*, 1096–1100.

(16) Li, X., Lee, J. S., Kraatz, H.-B. (2006) *Anal. Chem. 78*, 6096–6101.

(17) Drummond, T. G., Hill, M. G., Barton, J. K. (2003) *Nature Biotechnol. 21*, 1192–1199.

(18) Boon, E. M., Salas, J. E., Barton, J. K. (2002) *Nature Biotechnol. 20*, 282–286.

(19) Derosa, M. C., Sancar, A., Barton, J. K. (2005) *Proc. Natl. Acad. Sci. U.S.A. 102*, 10788–10792.

(20) Boal, A. K., Yavin, E., Lukianova, O. A., O'Shea, V. L., David, S. S., Barton, J. K. (2005) *Biochemistry 44*, 8397–8407.

(21) Gorodetsky, A. A., Boal, A. K., Barton, J. K. (2006) *J. Am. Chem. Soc. 128*, 12082–12083.

(22) Li, C. Z., Long, Y. T., Lee, J. S., Kraatz, H. B. (2004) *Chem. Commun. 7*, 574–575.

(23) Masarik, M., Cahova, K., Kizek, R., Palecek, E., Fojta, M. (2007) *Anal. Bioanal. Chem. 388*, 259–270.

(24) Kelley, S. O., Jackson, N. M., Hill, M. G., Barton, J. K. (1999) *Angew. Chem. Int. Ed. 38*, 941–945.

(25) Drummond, T. G., Hill, M. G., Barton, J. K. (2004) *J. Am. Chem. Soc. 126*, 15010–15011.

(26) Liu, T., Barton, J. K. (2005) *J. Am. Chem. Soc. 127*, 10160–10161.

(27) Inouye, M., Ikeda, R., Takase, M., Tsuri, T., Chiba, J. (2005) *Proc. Natl. Acad. Sci. U.S.A. 102*, 11606–11610.

(28) Boon, E. M., Jackson, N. M., Wightman, M. D., Kelley, S. O., Barton, J. K., Hill, M. G. (2003) *J. Phys. Chem. B 107*, 11805–11812.

(29) Di Giusto, D. A., Wlasoff, W. A., Giesebrecht, S., Gooding, J. J., King, G. C. (2004) *J. Am. Chem. Soc. 126*, 4120–4121.

(30) Di Giusto, D. A., Wlasoff, W. A., Giesebrecht, S., Gooding, J. J., King, G. C. (2004) *Angew. Chem. Int. Ed. 43*, 2809–2812.

(31) Zuo, X., Song, S., Zhang, J., Pan, D., Wang, L., Fan, C. (2007) *J. Am. Chem. Soc. 129*, 1042–1043.

(32) Okamoto, A., Kamei, T., Tanaka, K., Saito, I. (2004) *J. Am. Chem. Soc. 126*, 14732–14733.

(33) Okamoto, A., Kamei, T., and Saito, I. (2006) *J. Am. Chem. Soc. 128*, 658–662.

(34) Tanabe, K., Iida, H., Haruna, K., Kamei, T., Okamoto, A., Nishimoto, S. (2006) *J. Am. Chem. Soc. 128*, 692–693.

(35) Wang, A. H.-J., Gao, Y.-G., Liaw, Y.-C., Li, Y.-K. (1991) *Biochemistry 30*, 3812–3815.

(36) Leng, F., Savkur, R., Fokt, I, Przewloka, T, Priebe, W., Chaires, J. B. (1996) *J. Am. Chem. Soc. 118*, 4731–4738.

(37) Anne, A., Demaille, C. (2006) *J. Am. Chem. Soc. 128*, 542–557.

(38) Lai, R. Y., Lagally, E. T., Lee, S.-H., Soh, H. T., Plaxco, K. W., Heeger, A. J. (2006) *Proc. Natl. Acad. Sci. U.S.A. 103*, 4017–4021.

(39) Xiao, Y., Lubin, A. A., Baker, B. R., Plaxco, K. W., Heeger, A. J. (2006) *Proc. Natl. Acad. Sci. U.S.A. 103*, 16677–16680.

(40) Yavin, E., Stemp, E. D. A., O'Shea, V. L., David, S. S., Barton, J. K. (2006) *Proc. Natl. Acad. Sci. U.S.A. 103*, 3610–3614.

(41) Baik, W., Luan, W., Lee, H. J., Yoon, C. H., Koo, S., Kim, B. H. (2005) *Can. J. Chem. 83*, 213–219.

(42) Bondarev, G. N., Burzina, T. S., Krasotskaya, G. I., Kachurin, A. M., Kleiner, A. R. (1985) *Izvestiya Akademii Nauk SSSR: Seriya Khimicheskaya.* 1850–1855.

(43) Gannett, P. M., Darian, E., Powell, J. H., Johnson, E. M. (2001) *Synth. Commun. 31*, 2137–2141.

(44) Kelley, S. O., Barton, J. K., Jackson, N. M., Hill, M. G. (1997) *Bioconjugate Chem. 8*, 31–37.

(45) Gasper, S. M., Schuster, G. B. (1997) *J. Am. Chem. Soc. 119*, 12762–12771.

(46) Williams, T. T., Dohno, C., Stemp, E. D. A., Barton, J. K. (2004) *J. Am. Chem. Soc. 126*, 8148–8158.

(47) Shao, F., Augustyn, K., Barton, J. K. (2005) *J. Am. Chem. Soc. 127*, 17445–17452.

(48) Rist, M., Amann, N., Wagenknecht, H.-A. (2003) *Eur. J. Org. Chem*. *13*, 2498–2504.

(49) Abou-Elkhair, R. A. I., Netzel, T. L. (2005) *Nucleosides Nucleotides Nucleic Acids 24*, 85–110.

(50) Bard, A. J., Faulkner, L. R. (2001) *Electrochemical Methods*, *2nd ed*., John Wiley & Sons: New York.

(51) Geneste, F., Moinet, C. (2005) *New J. Chem. 29*, 269–271.

(52) Geneste, F., Moinet, C., Ababou-Girard, S., Solal, F. (2005) *New J. Chem. 29*, 1520–1526.

(53) Kelley, S. O., Barton, J. K., Jackson, N. M., McPherson, L. D., Potter, A. B., Spain, E. M., Allen, M. J., Hill, M. G. (1998) *Langmuir 14*, 6781–6784.

(54) Boon, E. M., Sam, M., Barton, J. K., Hill, M. G., Spain, E. M. (2001) *Langmuir 17*, 5727–5730.

(55) Oliveira Brett, A. M., Chiorcea, A.-M. (2003) *Langmuir 19*, 3830–3839.

(56) Rant, U., Arinaga, K., Fujita, S., Yokoyama, N., Abstreiter, G., Tornow, M. (2004) *Nano Lett. 4*, 2441–2445.